Australian Government
Department of Defence
Defence Science and
Technology Organisation

May 2004

DSTO

Evaluation of a Silent Killer, the PMN Anti-Personnel Blast Mine

R.J. Swinton and D.M. Bergeron

DSTO-TR-1582

Australian Government
Department of Defence
Defence Science and
Technology Organisation

Evaluation of a Silent Killer, the PMN Anti-Personnel Blast Mine

R.J. Swinton and D.M. Bergeron

Weapons Systems Division
Systems Sciences Laboratory

DSTO-TR-1582

ABSTRACT

The destructive output of the PMN mine was assessed experimentally by detonating actual mines in air and then in soil. The fragmentation pattern was recorded using a combination of flash X-rays, fragmentation packs, and gelatine cylinders. This made it possible to measure the velocity as well as the mass of the fragments, so that their injury potential could be estimated. This report describes the test set-ups and methodology used for the tests, and presents the results that were obtained.

Published by

DSTO Systems Sciences Laboratory
PO Box 1500
Edinburgh South Australia 5111 Australia

Telephone: (08) 8259 5555
Fax: (08) 8259 6567

AR-013-112
May 2004

APPROVED FOR PUBLIC RELEASE

Evaluation of a Silent Killer, the PMN Anti-Personnel Blast Mine

Executive Summary

The injury potential of the PMN anti-personnel blast mine was assessed experimentally using a range of diagnostics including flash x-rays, break screens, fragmentation packs, and gelatine semi-cylinders. Mines were first detonated in air to measure the maximum fragment velocity and maximum expansion rate of the detonation products that the mine could produce. Subsequent mines were detonated in soil to assess what effect this had on the mine blast and fragmentation outputs.

The detonations in air demonstrated that this mine produces significant fragmentation, due to the break up of the Bakelite case and the steel band that attaches the rubber cap and pressure plate to the main body of the mine. The steel band pieces had a mass up to 0.1 gram and could reach a velocity up 1100 m/s. The Bakelite fragments had an average mass around 0.2 gram and could reach a velocity between 1400 and 1800 m/s. The Bakelite fragments were uniformly distributed across an arc originating at the centre of the mine and about the horizontal plane. The steel band fragments were concentrated in the upper 5 degrees of this arc. Several fragments, originating from the pressure plate and the bottom of the mine were projected in the upward and downward vertical direction, respectively. The early expansion rate of the blast front had an initial velocity around 2000 m/s, which represents a significant overpressure for any object within 5 to 10 mine diameters from the mine.

Soil had a strong influence on the characteristics of the fragmentation and blast of the mine. The expansion rate of the detonation products was slowed down to around 900 m/s. In the immediate vicinity of the mine, the strong shock wave compressed the sand into a soft rock. The portion of soil immediately above the mine formed a crust that broke up into smaller fragments. These fragments had high momentum, creating impact craters that were up to 15 mm in diameter and 5 to 6 mm deep in aluminium. The flash x-rays revealed that the initial velocity of the ejecta front was of the order of 800 to 900 m/s. The velocity of the front of soil particles was highest in the vertical direction and dropped rapidly with increasing angle about the vertical axis.

In-soil detonations of PMN mines created a significant hazard to a contralateral leg placed 320 mm away from the mine. Gelatine semi-cylinders were damaged by the high-speed soil particles, which had an eroding effect on the skin and the underlying gelatine. For some tests, fragments from the mine case and from the steel band were embedded in the leg surrogates. It was however encouraging to note that this erosion of the soft tissues could be stopped by a few layers of soft armour.

Authors

R.J. Swinton
Weapons Systems Division

Robert Swinton joined DSTO in 1967 and has specialised in explosive analysis, testing, sensitivity/hazard assessment, and device development. He is currently working in the Countermine Technology Group investigating land mine effects and associated countermeasures.

D M. Bergeron
Weapons Systems Division

Dr Denis Bergeron joined Defence R&D Canada (DRDC) Suffield in 1983. He was project scientist for DRDC research in mine neutralisation and mine effects from 1995 to July 2002 when he started a 2 year attachment with DSTO Edinburgh, where he is conducting research in mine protection and blast physics.

Contents

1. INTRODUCTION 1

2. TEST SET-UPS AND METHODOLOGY 2
   - 2.1 Mines and Surrogate Charges 2
   - 2.2 Diagnostics 3
     - 2.2.1 Flash x-ray photography 3
     - 2.2.2 Break screens 3
     - 2.2.3 Caneite® packs 4
     - 2.2.4 Gelatine surrogates 4
   - 2.3 Set-up for the Air Blast Tests 4
   - 2.4 Set-up for the In-Soil Tests 6

3. RESULTS AND DISCUSSION 7
   - 3.1 Air Blast Test Results 7
     - 3.1.1 Expansion of the Detonation Products 7
     - 3.1.2 Fragment Velocity 9
     - 3.1.3 Fragment Dispersion 10
   - 3.2 In-Soil Test Results 12
     - 3.2.1 Expansion of the Detonation Products and Soil Ejecta 12
     - 3.2.2 Radial Expansion of the Soil Ejecta Front 14
     - 3.2.3 Fragmentation Hazard 16
     - 3.2.4 Simulation of a Polycarbonate Cylinder Impact on Aluminium 19
     - 3.2.5 Damage to the Gelatine Semi-Cylinders 20

4. DISCUSSION AND CONCLUSIONS 21

5. REFERENCES 23

APPENDIX A: DAMAGE REPORT FOR SEMI-CYLINDERS 25
- A.1. Tests 313-5: Unprotected target (Surrogate/TNT deflagration) in air initiation of PMN 25
- A.2. Tests 313-6: Unprotected target (PMN/PE4 filled) in soil initiation of PMN 26
- A.3. Tests 313-7: Single unprotected target (PMN/PE4) 27
- A.4. Tests 313-8: Unprotected target (PMN/TNT) 28
- A.5. Tests 313-8: Protected target (PMN/TNT) 29
- A.6. Tests 313-9: Unprotected target (PMN/TNT) 30
- A.7. Tests 313-9: Protected target (PMN/TNT) 31

1. Introduction

The PMN mine was developed in the early 1960s by the former Soviet Union. Countries including China and Hungary produced similar clones. Its large explosive content, 240 g TNT, earned it the reputation of being one of the most deadly anti-personnel (AP) blast mines ever deployed. It invariably leads to the traumatic amputation of the initiating foot and lower leg, severe injuries to the groin, lower abdomen, genitals and lower buttocks, the latter being areas where blood loss is very difficult to treat in the field. The contra-lateral leg (the non-initiating leg) is often injured as well. The extent of trauma that the PMN mine inflicts makes it the 'goal to reach' when designing protective measures.

The design of the PMN is simple and it is relatively inexpensive to produce, which might explain why it is widely deployed. Jane's [1] describes it as having a Bakelite body with a flat rubber pressure plate, reinforced by a Bakelite disc, and secured by a thin metal band. The fuze runs transversely through the mine body, with the arming delay assembly and arming pin protruding from one side and the detonator/booster assembly from the other. Figure 1 shows a sectioned diagram reproduced from [1]. The manufacturers also produced a modified version for booby-trap purposes (called the MS-3) such that the mechanism functions when a load is removed from the pressure plate.

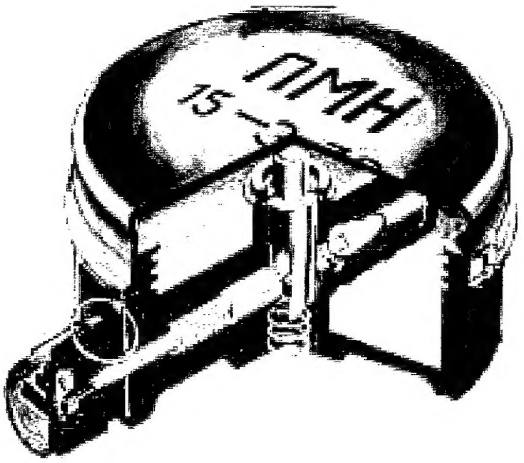

Figure 1. Sectioned diagram of a PMN mine showing the plunger and striker mechanism, reproduced from [1].

Anecdotal stories commonly refer to the PMN mine as being able to produce very energetic fragments. This might be attributed to the thick Bakelite casing and metallic components, which have the potential of producing a substantial fragmentation hazard within a few metres. A proper evaluation of the blast field and fragmentation pattern of the PMN was therefore warranted; hence DSTO performed such an evaluation to

quantify the destructive output of the PMN mine. The resulting information can be important in several areas:

- The design of protective footwear and clothing
- Advice relating to mine clearance
- Development of neutralisation devices
- Recommendations for medical treatment
- Establishment of safety distances

2. Test Set-ups and Methodology

In order to characterise the output of the PMN mine, it is necessary to quantify the threats posed by fragmentation and by blast. The fragmentation characteristics can be determined by measuring the range of fragment sizes and their initial velocity. The overall distribution in space, i.e., where the fragments go, should also be measured. However, it is well known that the soil influences the path and velocity of fragments; hence an explosion in air, when the mine is fully exposed, provides an upper limit to the fragmentation threat. It was also decided to measure the fragmentation threat when the mine is buried, since this is very relevant to the design of protective equipment and to assess the potential of injury. In this case, soil ejecta also pose a significant fragmentation threat to a person close to the explosion.

The traditional method to assess the blast threat is to measure the blast overpressure field around the source of the explosion. However, for AP mines, it is not sufficient to measure blast overpressure [2,3,4] because a large portion of the pressure felt on the body surface is also due to the flow of detonation products and multiple impacts from soil particles, the latter causing erosion of soft tissue. A proper assessment of blast means that these quantities must also be measured. The flow velocity can be assessed using photographic methods, while the erosion from soil particles impacts can be assessed from their effect on a structure that is representative of the human body.

2.1 Mines and Surrogate Charges

Only four complete PMN mines were available for these tests. In addition, three PMN mine cases that had the explosive removed were also on hand. One of these cases was refilled with cast TNT while the other two cases were filled with 200 grams of PE4 plastic explosive. Given the very limited number of mines, it was important to plan the test set-ups carefully and to optimise the diagnostics for each shot. Two mines were used for the air blast tests and all others were used for the in-soil tests.

In order to finetune the diagnostics and test methodology, four surrogates of the PMN mine were constructed from a PVC pipe and other plastic components. The height and

diameter of the surrogates were the same as those of the mine. Three of these surrogates were filled with 240-280 grams of cast TNT while the fourth was kept inert for use during test preparations. The surrogates included a transverse fuze well similar to that of the real mine. The detonation of the mines and surrogates was initiated with a Reynolds 501 series detonator and 10 to 15 grams of PE4 packed in the fuze well. This was deemed to best reproduce the actual way that the mine functions.

2.2 Diagnostics

Four diagnostics tools were used throughout this test series. These were flash x-ray radiography, break screens, Caneite® fragmentation packs, and purpose-made gelatine semi-cylinders. A more detailed description of each diagnostic method is provided below while their placement within the test chamber is explained later in Sections 2.2 and 2.3 for the tests in air and in soil, respectively. All tests were performed in blast chamber no. 2 of the High Explosive Facility Complex at DSTO Edinburgh, Australia.

2.2.1 Flash x-ray photography

Two 300 kV flash x-ray heads were used to capture the early explosion process of the mines. When the mine detonation occurred in air, the x-rays provided a measure of the fragment distribution and the shape of the detonation products. The velocity of the fragments could be measured from two successive radiographs. When the mine was buried in soil, the radiographs captured the position of the front of detonation products, the shape of the cloud of detonation products, and the dispersion of soil particles. The timing of the radiographs was varied in order to determine the time history of the front, from which velocity could be computed.

2.2.2 Break screens

The break screens had a total frontal area of 830 mm in height and 180 mm in width. This area contained four sensing sections that were 150 mm in width with variable heights, starting from the bottom, of 240 mm, 190 mm, 140 mm, and 180 mm, respectively. These dimensions crudely represented different regions of the human leg, (being the foot-to-ankle, ankle-to-calf, calf-to-knee and knee-to thigh). The 0.29 mm thick enamelled copper break wires were wound at a 1 mm interval along the front and rear of a wooden frame. This was done by inserting 1 mm thick printed circuit board terminal pins in accurately drilled holes at 2 mm intervals and winding the wire back and forth across the screen. The wires were tensioned before each shot by tightening three screws on the side of the wooden frame. The distance between the leading edge of the front and back wires was 50 mm. Two oscilloscopes were used to time when each of the eight wires (4 front and 4 back) broke after the detonation pulse. During the air detonations, the mine fragments' path was roughly aligned with the depth of the break screens, hence the velocity was directly proportional to the separation distance between corresponding screens. For tests where the detonation occurred in soil, the break screens were placed upright along side the soil container,

with the base at the same height as the soil surface. In these tests, the soil particles and fragments travelled at an angle about the vertical, which had to be accounted for when computing the velocity of the particle front.

2.2.3 Caneite® packs

During the air detonation tests, Caneite® was used to 'soft recover' the fragments generated by the break-up of the mine casing. These Caneite® fragmentation packs were constructed by stacking five 12.7 mm thick sheets that had a surface area of 915 mm × 915 mm. Masking tape wrapped around each pack held them together. They were then mounted to the wall of the blast chamber. An early attempt was made to place the packs closer to the mine, but this was abandoned immediately. The force of the blast, combined with the high concentration of fragments destroyed the packs, which made analysis of fragment distribution extremely difficult.

Fragments were also recovered by sifting the sand after an experiment, including the sand that was recovered from the chamber floor. This method proved very efficient and yielded a large number of fragments that were sufficiently well preserved for inspection at a later time.

2.2.4 Gelatine surrogates

On request, Anatomical Surrogate Technologies (AST) [5] manufactured for these experiments basic 'soft target' surrogates to represent a human lower leg (at a length of 640 mm) by using ballistic gelatine that was coated with a chamois to simulate the skin. These surrogates were cast into a 150 mm diameter semi cylinder mould in which the chamois material had been placed such that it over hung on both sides. After setting, a 10 mm thick plywood sheet was placed on the flat back, the chamois skin was stretched across the plywood sheet, and it was finally stapled in place. The entire target was then placed into a heavy gauge stocking and secured at both ends. AST was also contracted to perform the post-test forensic analysis, which included providing x-rays, and then performing a physical dissection and inspection.

2.3 Set-up for the Air Blast Tests

Figure 2 shows a plan view of the test set-up used for the air blast tests. The charge was suspended from the ceiling using a nylon stocking and rope, as shown in Figure 3. It was located 1.26 m above the floor at the intersection of two sight lines for the flash x-ray equipment. The existing portholes in the walls of the chamber fixed the height. Two individual x-ray cassettes were supported on top of the shelf of a rigid steel table. The table had been manufactured specifically to hold a soil container at the correct height for flash x-ray radiography. A single sheet of Caneite® placed behind a single sheet of 6 mm thick polycarbonate was taped to the front of each cassette in order to prevent fragment penetration. The cassettes were located such that the distance from the centre of the mine to the film was 600 mm. This gave a magnification factor of 1.22.

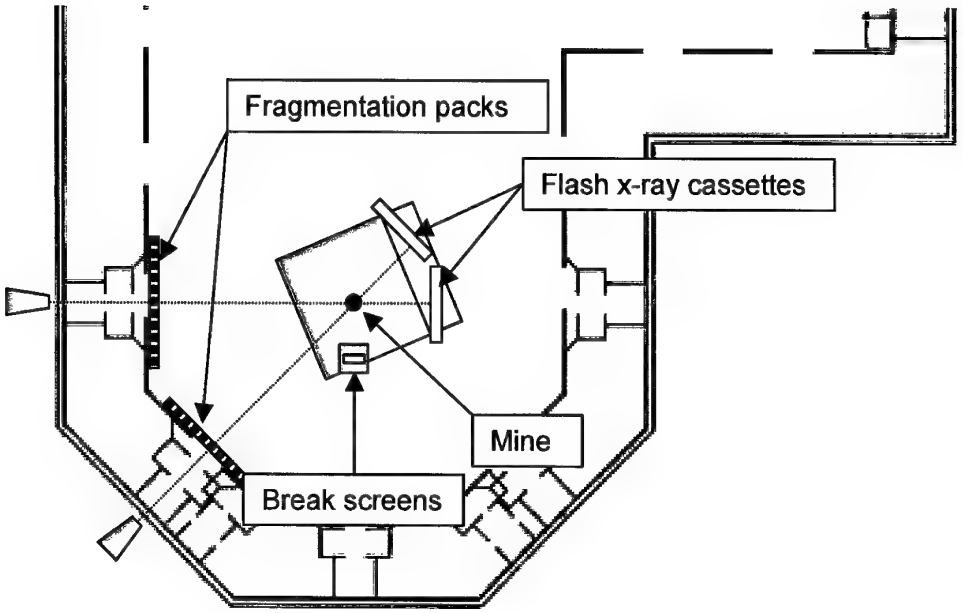

Figure 2. Plan view of the set-up used for the air blast tests of the PMN mines.

The break screens were placed 345 mm from the centre of the mine. Each break screen rested on top of the table surface so that the centre of the second sensing section of the break screen (from the bottom) would be at the same height as the mine body. This height made best use of three of the four sensing sections. Finally, the Caneite® packs were loosely attached to the walls of the chamber 1.35 m away from the mine. The centre of the packs (along the black line) was positioned at the same height as the mine body. Figure 3 provides more details of the test set-up.

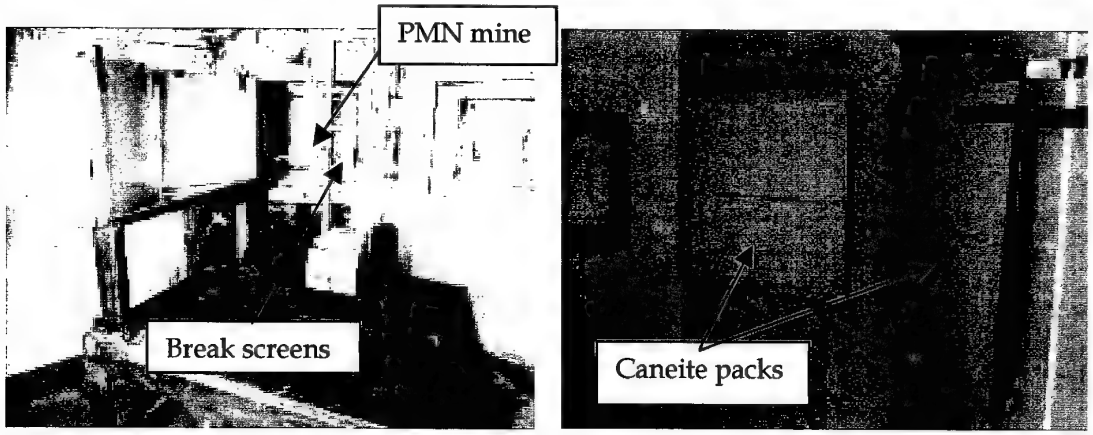

Figure 3. Details of the set-up showing (left) the PMN mine suspended above the table with break screens and flash x-ray cassettes and (right) Caneite® packs on the wall.

2.4 Set-up for the In-Soil Tests

Figure 4 shows a plan view of the test set-up used when the mines were buried in soil. A steel container 800 mm in diameter and 500 mm deep was located on top of the steel table such that its centre was directly below the intersection of the flash x-ray sight lines. The container was filled with dry medium sand that had a bulk density of 1.63 g/cc. The sand was levelled to the rim prior to each test. Following a test, contaminated sand was removed and replaced with fresh sand. The mines were buried at the centre of the container such that the top was 20 mm below the surface. This is consistent with a test methodology that has been proposed by NATO [6].

The diagnostics consisted of break screens, gelatine semi-cylinders, and flash x-ray radiography. In addition, some of the gelatine semi-cylinders were used to assess various flexible materials that could be used to construct protective gaiters. The break screens were located back to the edge of the container, placing the front face 400 mm from the centre axis of the mine. Two gelatine semi-cylinders were tied in a vertical position on opposite sides of the soil container, placing their face 325 mm away from the centre axis of the mine. A single purpose-built cassette that contained two films at 45-degree angle replaced the two individual flash x-ray cassettes used during the air blast tests. The design of this purpose-built cassette was such that the distance from the centre of the mine to the films remained at 600 mm, thereby maintaining the magnification factor of 1.22. Figure 5 shows more details about this test set-up.

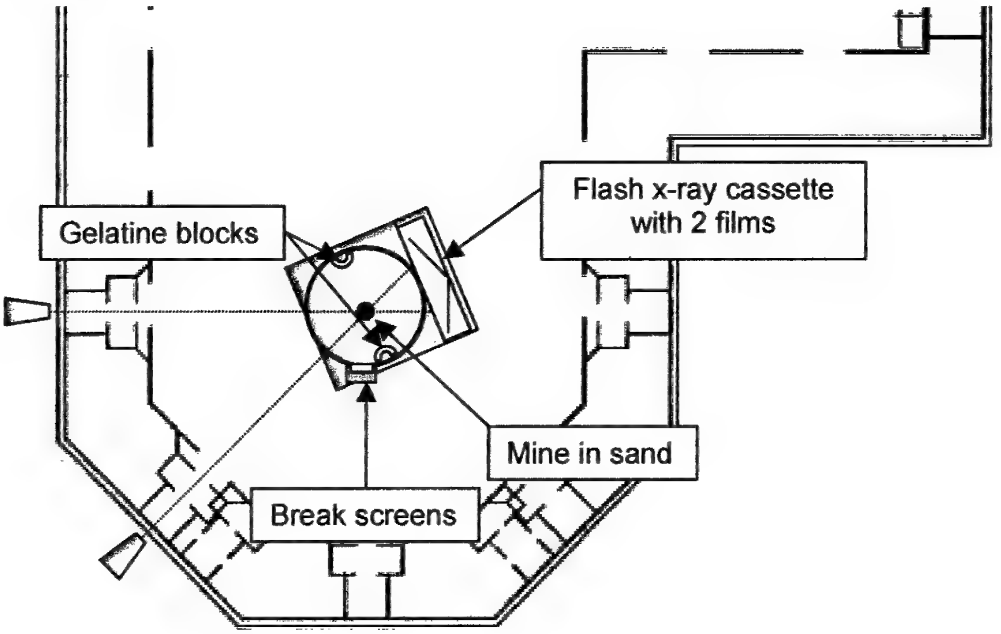

Figure 4. Plan view of the set-up used for the in-soil tests of the PMN mines.

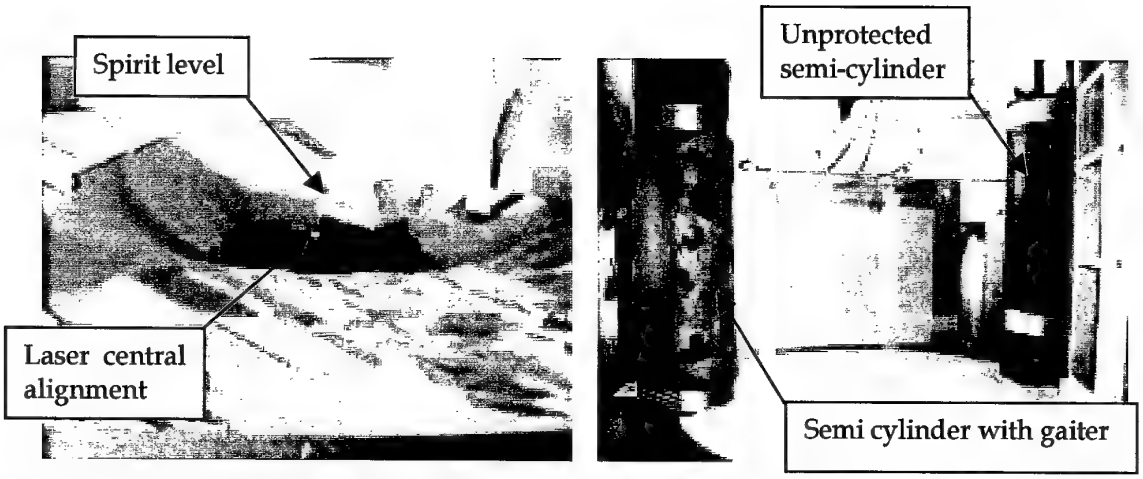

Figure 5. Details of the in-soil set-up showing (left) burial of the PMN mine and (right) flash x-ray cassette, gelatine semi-cylinders and break screens.

3. Results and Discussion

3.1 Air Blast Test Results

The results from the air blast tests are divided into two elements. First, it is of interest to consider the shape of the cloud of detonation products and the rate of its expansion. Second, the fragment distribution and fragment speed need to be quantified. This information was derived from analysis of the flash x-ray records, the velocity screens' timings, and visual inspection of the Caneite® fragmentation packs.

3.1.1 Expansion of the Detonation Products

Figure 6 presents three flash x-ray records obtained from detonations of the PMN mine in air. The timing for these records were 21.2 μs, 61.2 μs, and 100.8 μs, respectively. During the second test, the x-ray films (left and right pictures in Figure 6) were exposed twice, a first time to mark the location of the mine in the field of view, and the second time to capture the location of the detonation products and fragments after detonation. During the first test, fragmentation packs were placed close to the mine; these show up as white vertical bands on the left hand side of the centre picture in Figure 6.

It is seen from Figure 6 that the cloud of detonation products had just crossed the physical bounds of the mine body at 21.2 μs, but that it expanded rapidly thereafter. The shape of the cloud was roughly symmetrical about the vertical axis. There was also a stronger flow of detonation products in the vertical and radial directions, while the flow at the ±45-degree azimuths clearly exhibited a velocity deficit. These characteristics are due to the cylindrical geometry of the explosive.

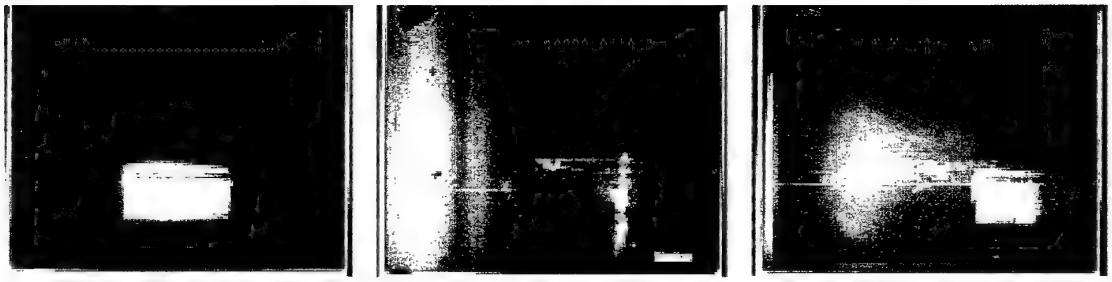

Figure 6. Flash x-ray radiographs of PMN mine explosion in air at (left) 21.2 μs, (centre) 61.2 μs, and (right) 100.8 μs; Left and right pictures were double exposed to mark the location of the mine.

Three series of points were extracted from the radiographs, which corresponded to the leftmost positions of the detonation products and metal band in the radial direction, and the highest position of the detonation products in the vertical direction. It should be noted that the upper edge of the detonation products was beyond the boundary of the radiograph at 100.8 μs and that corrections were applied to account for variations in the initial position of the mine from one test to the next. The corrected data is plotted in Figure 7. Using linear least square fits, the average velocity during the early expansion of the detonation products was measured to be 1950 m/s in the radial direction and 2110 m/s in the vertical direction. The edge of the metal band followed a path that is inclined upward by approximately 15 to 20 degrees relative to the horizontal. The average velocity of these fragments was 1140 m/s.

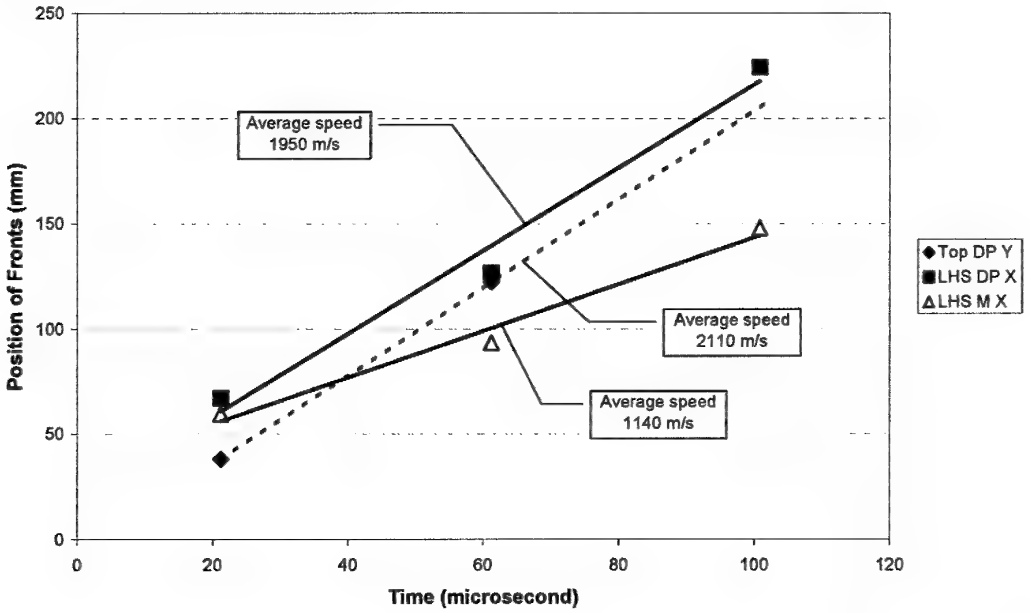

Figure 7. Position of the fronts of detonation products (radial left and vertical top) and of the leftmost side of the expanding metal band of the mine.

3.1.2 Fragment Velocity

The fragment velocity was determined from two sources. First, the flash radiographs show that the front of the steel band had moved 91 mm between two successive frames taken 79.6 μs apart, which corresponds to 1143 m/s. The second method used to measure fragment velocity was the break screens. The front and rear screens were spaced 50 mm apart, however, given the test set-up, the fragments did not usually travel exactly in the direction perpendicular to the break screens. Figure 8 shows the geometry of the set-up and shows the minimum and maximum angles of fragment travel for each screen pairs. These angles are listed in Table 1 (on following page). Dividing the minimum and maximum path lengths by the time difference for corresponding screen breaks yields a velocity range for each screen segment, as listed in Table 1.

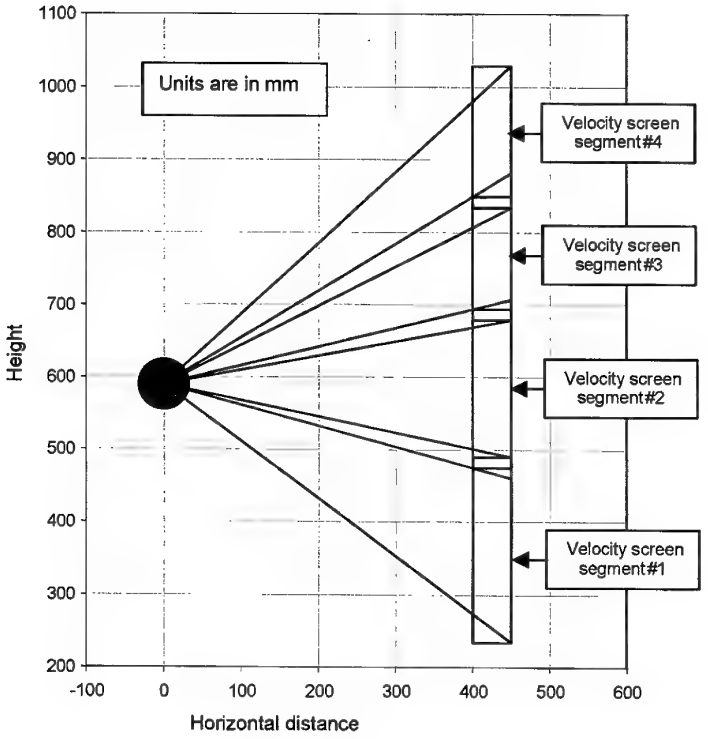

Figure 8. Shot lines for the break screens give a range of fragment velocities.

There were differences in fragment velocity between tests 313-2 and 313-3. These were only of the order of 10-12% for segment # 2, but were much greater, up to a factor of 1.9 for the adjoining segments. The fastest fragments crossed the screen segments # 2 with a velocity ranging from 1416 to 1601 m/s. This is higher than the velocity of the metal band measured on the x-rays, but lower than the corresponding radial velocity of the expanding detonation products. This suggests that the Bakelite fragments lagged the

detonation products and caused the breaks in segment # 2. The metal band likely crossed the upper portion of segment # 2 or the lower portion of segment # 3. The velocity for this last segment ranged from 760 to 1293 m/s, which appears consistent with the passage of the metal band.

An alternate method to estimate fragment velocity is from the time when the front screens broke. It is seen from Table 1 that this time was consistent from test to test, being 220 and 228 μs for screen # 2. By deducting the time required to complete the detonation process and break up the case (approximately 20 μs) from these timings, and knowing that the minimum distance between the edge of the mine and the front of that screen was 345 mm, the velocity was estimated to range from 1660 to 1725 m/s, which appears to be consistent with the passage of the Bakelite fragments.

Table 1. Velocity screen results for air blast tests of PMN mine.

Test ID	Screen #	θ_{min}	θ_{max}	t_{front}	t_{back}	V_{min}	V_{max}
		(Deg)	(Deg)	(μsec)	(μsec)	(m/s)	(m/s)
313-2	1	-38.3	-16.2	320	496	296	362
	2	-12.7	11.2	228	260	1563 *	1601
	3	14.6	28.5	272	316	1174	1293
	4	32.9	44.3	288	2352	29	34
313-3	1	-38.3	-16.2	272	364	566	693
	2	-12.7	11.2	220	256	1416	1423
	3	14.6	28.5	260	328	760	836
	4	32.9	44.3	284	N/R	N/R	N/R

Notes: N/R: not recorded since no pulse was generated.

Screen # 1 is the lowest and # 4 is the highest.

* The shortest path for screen # 2 is 50 mm, which gives the lower velocity limit.

3.1.3 Fragment Dispersion

The Caneite® packs at the wall were successful in capturing the pattern of dispersion of the mine fragments as well as recovering some fragments. Figure 9 shows the front face of the first and second sheets of the left and right fragment packs. The horizontal line on the first sheets indicates the height of the mine body at the time of detonation. It is clear from the front sheet that the PMN mine spreads numerous fragments over the ±19 degrees elevation arcs covered by the packs. It can also be seen that these fragments vary in size, as witnessed by differences in the diameter of the penetration holes. However, the majority of these fragments carry little penetration power as only a small fraction penetrated through the front sheet and into the second Caneite® sheet. A close examination of the impact points and recovery of some fragments confirmed that the majority of hits were from small Bakelite fragments. However, some holes also

contained bits of rubber from the mine cover. The larger Bakelite fragments, some with rubber, penetrated through the first sheet and were found embedded into the second sheet. In addition, a limited number of steel fragments from the band holding the rubber cap in place were found in the second sheet. Some metal fragments also had sufficient penetration power to penetrate through the second sheet and into the third and fourth sheets.

Figure 9. Front face of the first (top images) and second (lower images) sheets of the left and right Caneite® fragment packs showing the dispersion of the fragments.

These metal fragments had a width of 2-3 mm and varied in length from 2 mm up to 20 mm. Figure 10 shows examples of the more energetic fragments recovered in sheets 2 to 4 of the fragment packs. There was also a thin slit through sheet 5 of one pack, indicating that a thin metal strip had gone right through. This suggests that the strip hit the pack when on its side, acting like a razor blade to produce the most efficient penetration. The large majority of the metal strip fragments were found in the top 150 mm of the Caneite® sheets. This corresponds to an elevation angle between 13 and 19 degrees.

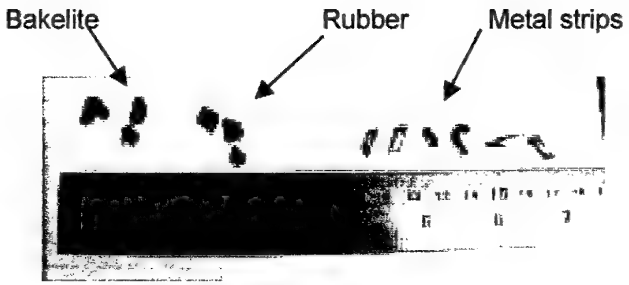

Figure 10. Fragments recovered from sheets 2 to 4 of the Caneite® packs.

3.2 In-Soil Test Results

A total of five tests were performed with buried mines. Three of these tests used PMN mines with a TNT fill, while the other two tests were performed with PMN mine bodies that had been refilled with 200 grams of PE4. As explained in section 2.4, the mines were buried under 20 mm of dry sand the data measured included flash radiography, break screens, and semi-cylinders of gelatine.

3.2.1 Expansion of the Detonation Products and Soil Ejecta

Figure 11 presents six radiographs of the expanding detonation products. Early on, it takes a finite amount of time, estimated to be between 30 and 50 μs, before any visible motion of the soil takes place. The soil cap then rises, taking a hemispherical shape.

The early radiographs show a region of high density directly above the mine. It is surmised that the soil was compressed into a 'solid cap' that broke up soon thereafter. Following each in-soil test, large chunks of white, rock-like material were recovered. This material was the original sand that had been shattered and highly compressed into a solid mass in the very near vicinity of the mine. Some authors refer to this region as the *region of crush* or *region of total destruction.* It is likely that the region of high density hides Bakelite and rubber fragments that came from the mine's pressure plate. In two radiographs, the shape of the fastening clip that normally holds the plunger in its cavity is seen flying upward. The later time radiographs still contain regions of high density, but overall, soil dispersion and venting of the gas are occurring.

The vertical position of the front of detonation products/soil ejecta was measured and plotted in order to determine velocity. Figure 12 shows the result. Lines connect the points that correspond to the same test and the average velocity for each pair is indicated. It is seen that the average velocity decreased as the average time increased. However, the points from successive tests do not intermesh properly. If they did, the point from test 313-8 at 151 μs would be sitting slightly to the left of the line joining the two points from test 313-9 (at 101 and 201 μs). These shifts in time suggest that there were variations in the time required to initiate the main charge of the mines. The three points from the mines filled with PE4 are collinear, which suggests that this was not as

much an issue for that explosive. Another point worth noticing with the PE4 test results is that the initial velocity was very close to that for the TNT tests. This suggests that the amount of explosive that was used was a suitable equivalent to the TNT fill.

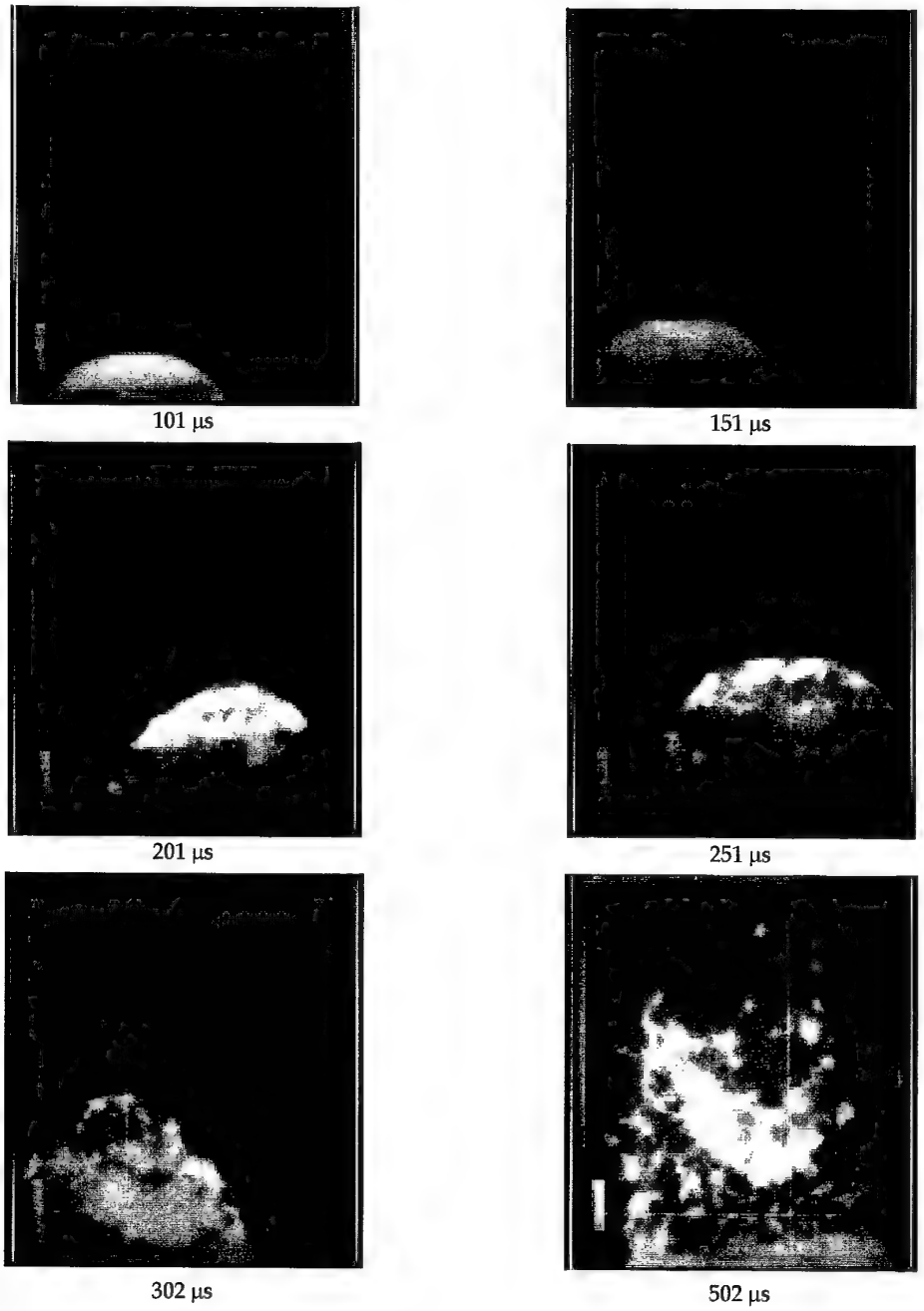

Figure 11. Flash x-ray radiographs of the expansion of the detonation products and soil ejecta for PMN mines buried under 20 mm of dry sand.

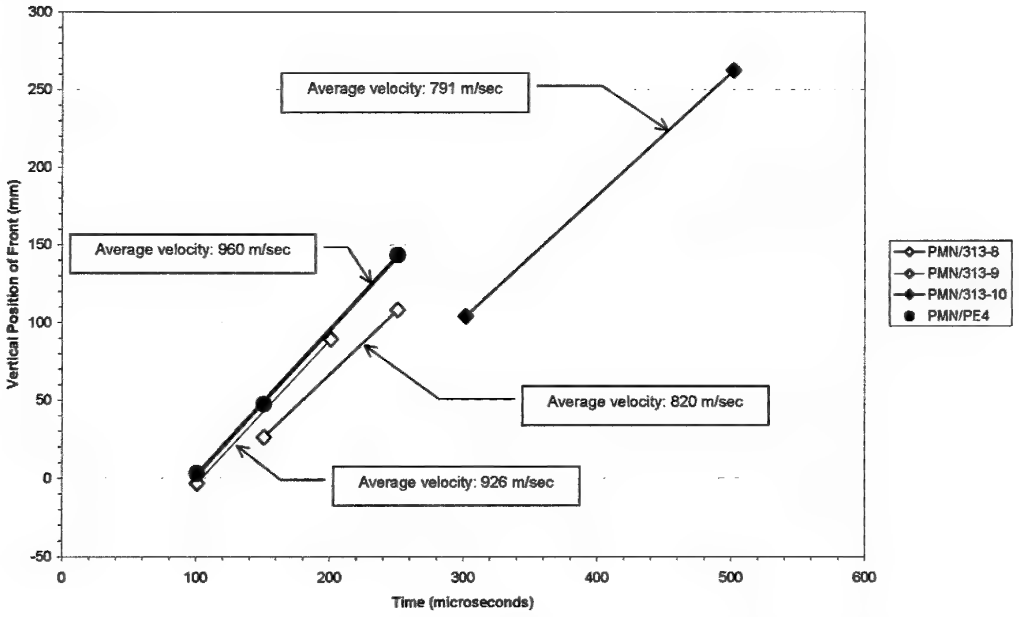

Figure 12. Vertical position of front of detonation products for PMN mines buried under 20 mm of sand; data also included PMN mine bodies filled with 200 grams of PE4.

3.2.2 Radial Expansion of the Soil Ejecta Front

The radiographs of Figure 11 show that the expansion of the soil cap is not uniform. There is a strong vertical component to the flow. By considering the position of the particle front on the radiograph at various times, it is possible to estimate the speed of advance of this front along any radial line about the centre of explosion. It should be noted that particles do not, in general, follow these radial lines, but tend to flow along paths that are more vertical. Nevertheless, knowing the radial progression of the front can be useful. Figure 13 shows a series of points corresponding to the particle front for two radiograph pairs. A third order polynomial curve was fit to each set of points in order to estimate the progression of the front along any radial between 30 and 90 degrees about the horizontal. This was achieved by computing the intersection between each of these polynomials and a straight line passing through the centre of explosion.

The result from the above computations is plotted in Figure 14. The reader should not attach any physical meaning to the variation of velocity between 70 and 90 degrees, as this is an artefact of the curve fit procedure. In fact, the radiographs indicate that the particle front velocity in the region directly above the top of the mine is relatively constant with a value near the larger velocity estimate of 884 m/s. Outside of the soil cap zone, the radial velocity of the front diminishes rapidly with decreasing angle.

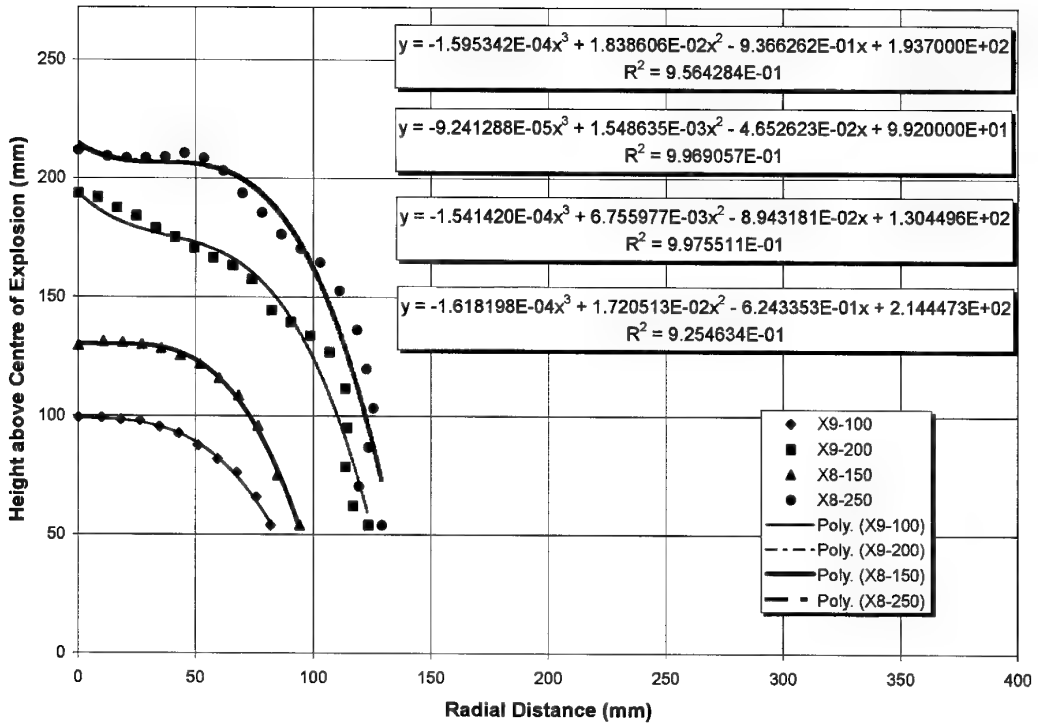

Figure 13. Position of the soil particle front with third order polynomial fits to estimate velocity.

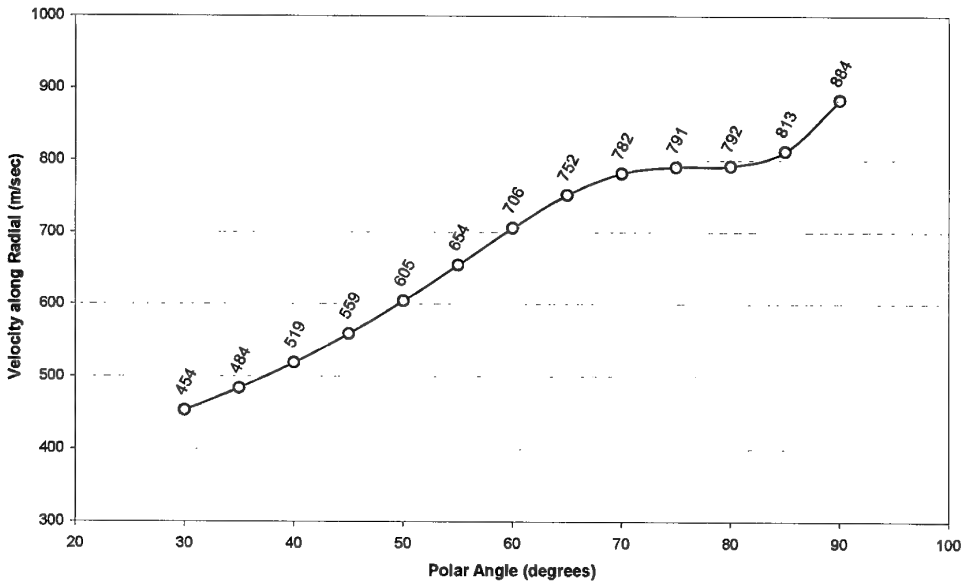

Figure 14. Estimate of the expansion velocity of the particle front as a function of radial angle.

3.2.3 Fragmentation Hazard

Since these tests were performed in a closed environment, significant portions of the fragments were recovered by sifting the sand left in the bucket and the debris from the chamber floor. Figure 15 shows the collection of fragments recovered from one test. The Bakelite fragments varied greatly in size and mass. The mean fragment mass was approximately 0.2 gram (~5 mm cube) and the larger fragments weighed roughly 1 gram. The steel strips were approximately 4 mm wide by 0.5 mm thick and varied in length from 3 to 17 mm, with mass from 0.025 to 0.125 g. The rubber pieces, which had penetrated into the second Caneite® sheet weighed between 0.03 and 0.06 g. An aluminium fragment that was recovered after shot 313-3, thought to have been part of the striker assembly, weighed approximately 2.5 g. After shot 313-8, another fragment of the striker assembly with spring (shown in Figure 15), was recovered, which weighed 3.5 g. Both these pieces had the steel firing pin section missing.

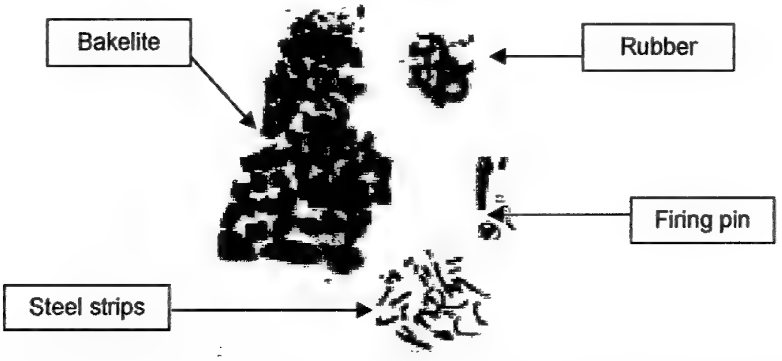

Figure 15. Fragments recovered from in-soil test after sifting sand and blast chamber debris.

It is therefore seen that the PMN mine generates a significant amount of fragmentation. Some fragments, such as the firing pin and portions of the mine case, are large and massive. Given sufficient velocity, such fragments are potentially lethal.

Figure 16 shows the result of multiple impacts from upward-flying fragments on the aluminium crossbar of the test rig. These impacts left craters that were up to 15 mm in diameter and 5 to 6 mm in depth. It is unclear whether these fragments originated from the original mine or from sand particles that had been compressed to the point of becoming soft rock. The larger craters were found within 120 mm from the centre of the crossbar, while smaller craters were seen along the full length of the 874 mm long bar. Thus, larger fragments hit within a 5-degree cone (included angle) while smaller fragments hit within a 30-degree (minimum) cone.

Analysis of the radiographs provided an upper limit of approximately 800 m/s for the vertical velocity. Drag and gravity have a minimal effect on this velocity over the 1.47 m height of the set-up. Unfortunately, the exact mass and geometry of the fragments is not known and further testing would be required to determine this.

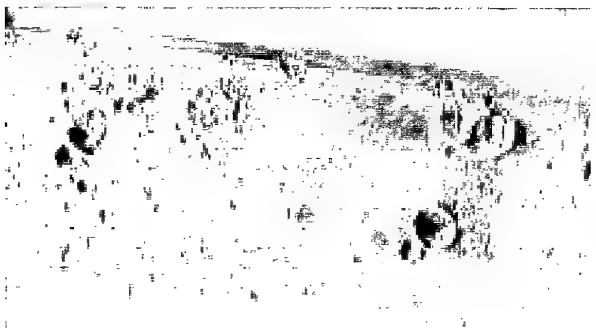

Figure 16. Impact craters from mine fragments into a 100 mm wide aluminium bar that was located 1.47 m directly above the surface of the sand.

The break screens also provided a measure of the velocity range at a lateral offset from the vertical axis. Figure 17 shows the position of the screens relative to the mine. It is seen that rays originating from the centre of explosion intersect the screens at angles ranging from 12 to 62 degrees from the horizontal.

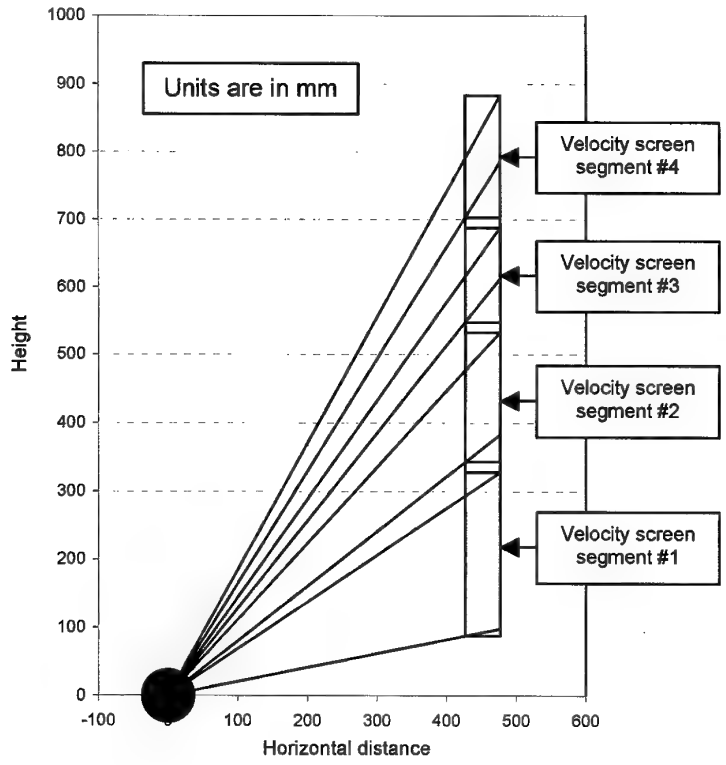

Figure 17. Shot lines for the break screens give a range of fragment velocities.

It is seen from Table 2 that the rear screen data was often lost. However, the front screen data was always captured. For those cases where both the front and rear screen data is available, the minimum (61 m/s) and maximum (805 m/s) velocities were both recorded with screen # 1 at the lowest height. The maximum velocity gradually decreased with height. Generally, there were large variations in the velocity estimates obtained from the time difference between corresponding front and rear screen breaks, which cast some doubt about using this measurement method for this particular scenario.

Table 2. Velocity screen results for in-soil tests of the PMN mine.

Test ID	Scrn #	θ_{min} (Deg)	θ_{max} (Deg)	t_{front} (μsec)	t_{back} (μsec)	V_{min} (m/s)	V_{max} (m/s)	Vf_{min} (m/s)	Vf_{max} (m/s)
313-6	1	12.0	35.2	904	N/R	N/R	N/R	469	562
	2	39.6	48.9	836	1000	396	464	644	755
	3	52.9	55.9	980	1472	168	181	701	756
	4	59.4	62.2	1172	N/R	N/R	N/R	697	760
313-7	1	12.0	35.2	844	1684	61	73	503	602
	2	39.6	48.9	888	1`044	416	488	606	711
	3	52.9	55.9	984	1168	450	485	699	753
	4	59.4	62.2	932	1420	202	220	876	956
313-8	1	12.0	35.2	832	N/R	N/R	N/R	510	610
	2	39.6	48.9	832	1180	186	219	647	646
	3	52.9	55.9	1064	N/R	N/R	N/R	646	697
	4	59.4	62.2	1244	N/R	N/R	N/R	656	716
313-9	1	12.0	35.2	692	840	345	413	613	734
	2	39.6	48.9	624	804	360	423	863	1012
	3	52.9	55.9	796	N/R	N/R	N/R	864	931
	4	59.4	62.2	1036	N/R	N/R	N/R	788	860
313-10	1	12.0	35.2	928	1004	673	805	457	547
	2	39.6	48.9	900	1012	579	679	598	701
	3	52.9	55.9	1020	1432	201	217	674	727
	4	59.4	62.2	1092	1816	136	148	748	816

Notes: N/R: not recorded since no pulse was generated.

Screen # 1 is the lowest and # 4 is the highest relative to the surface of the sand bucket.

If the time when the front screens broke is considered instead, the estimates of velocity are more consistent from one test to the next. These times were computed from the geometry, i.e., the 415 mm distance between the front break screens and the vertical axis through the centre of the mine, and the angle of the rays originating from the centre of explosion and intersecting each break screen pair. They are listed in Table 2.

Using the time of arrival at the front screens to compute average velocity yields values anywhere from 450 m/s up to 1000 m/s, but most of the data is between 600 and 700 m/s. There is also another trend in that the lowest velocity is recorded at the lowest screen segment and generally increases with height. This is consistent with the fact that the soil cap is being ejected at high speed in the vertical direction. The longer time to break the lowest front screen might be linked to the expansion of the crater radius, which occurs at a slower speed than the ejection of the soil cap. The break times for the front screens also appears to be consistent with the expansion of the soil cap alone, which suggests that it is mainly soil particles that break the screens.

3.2.4 Simulation of a Polycarbonate Cylinder Impact on Aluminium

The penetration potential of a plastic-like fragment into aluminium was investigated numerically using the LS-Dyna computer code. For simplicity, the computation considered the impact of a polycarbonate cylinder onto a cylinder of 6061 aluminium. Realizing that the impact dynamics is governed mainly from a local interaction between two materials, the numerical grid concentrated on the immediate zone around an impact point. The computation was performed in the axi-symmetric configuration. The polycarbonate cylinder was 10 mm in diameter and 10 mm long with a mass of 0.94 gram. These particular dimensions were selected to approximate the upper portion of the Bakelite plunger of the PMN mine. The aluminium cylinder was 20 mm in diameter and 25 mm thick. A fixed boundary condition was applied to the sidewalls of the cylinder. Two impact velocities were considered, 400 m/s and 800 m/s, which were consistent with the experimental observations.

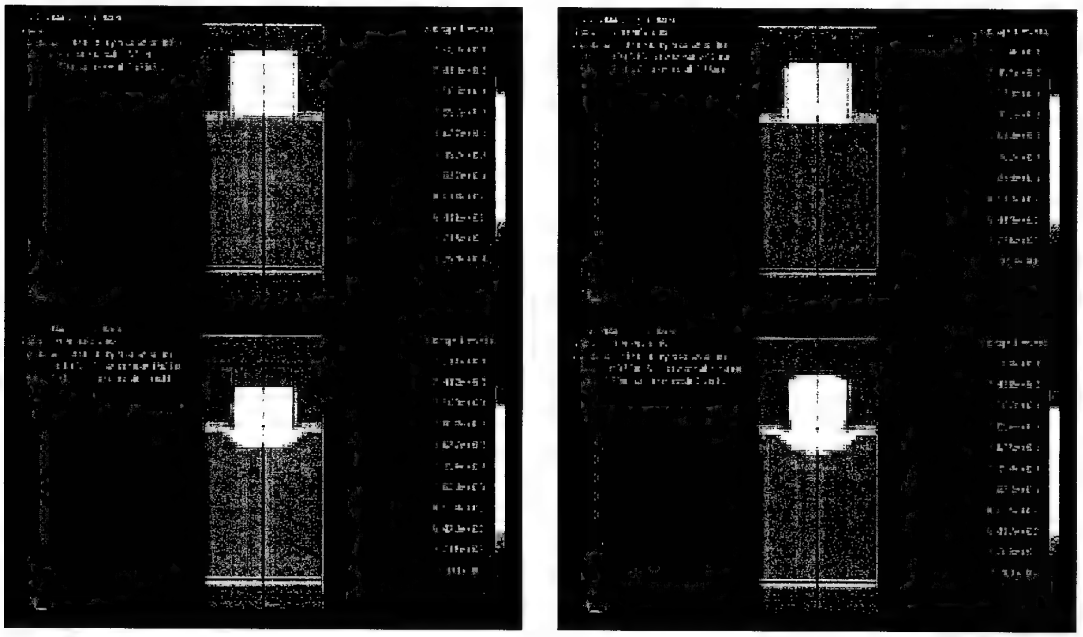

Figure 18. Density contours from LS-Dyna showing the penetration of a polycarbonate cylinder into 6061 aluminium. Maximum penetration was 3.4 mm.

Figure 18 shows a series of density contours for the 800 m/s case. The upper left picture shows the initial state of density at impact. The green colour corresponds to the density of polycarbonate (1196 kg/m^3) and the red colour to the density of aluminium (2703 kg/m^3). The results suggest that maximum penetration occurs within 10 to 20 μs from the time of impact. For an initial velocity of 800 m/s, the simulated impact creates a crater that is 13.5 mm in diameter and 3.4 mm deep. This is similar to the crater dimensions that were observed experimentally. The corresponding computation with an initial velocity of 400 m/s resulted in a crater that was only 1 mm deep.

3.2.5 Damage to the Gelatine Semi-Cylinders

A total of 7 gelatine semi-cylinders were used in the 5 in-soil tests. During test 313-5, which used a PMN surrogate, the explosive deflagrated instead of detonating, but since damage was inflicted to the semi-cylinder, this data is included below. The semi-cylinders were taped to the vertical frame of the firing rig, as shown in Figure 19, such that the curved skin-like surface was 320 mm from the vertical line extending through the centre line of the buried mines. Of the 7 targets, 2 were protected with an additional layer of ballistic soft armour constructed from layers of various Aramids. After the tests, the semi-cylinders were sent out to AST for examination, which included medical x-rays. The AST results and comments are reproduced in Appendix A. The reader should note that the x-rays had to be taken in two parts because the semi-cylinders were longer than the imaging window capability of the AST x-ray machine. Thus, Appendix A presents overlapping views of the same semi-cylinders, with the left views showing the upper segment of each semi-cylinder, and the right views showing the lower segment of the same semi-cylinder.

The semi-cylinders without protection all sustained significant damage, even for test 313-5 where the charge deflagrated. The damage consisted of a combination of skin tears and erosion of the underlying gelatine. This occurred between 100 and 200 mm from the base of the semi-cylinders, as can be seen in the post-test photo, of Figure 19. AST assessed that given the height of the damage, it was probable that the stress on the tibia could have exceeded the local bone strength and resulted in a break. In two subsequent tests, fragments were embedded in the upper portion of the semi-cylinders. In one case, the fragment was identified as a portion of the steel band holding the rubber cap on the mine body. For the two tests performed with soft armour, there was no visible damage to the semi-cylinders with the exception of blunt impact and possible friction. This suggests that this type of protective material is effective at the distance tested.

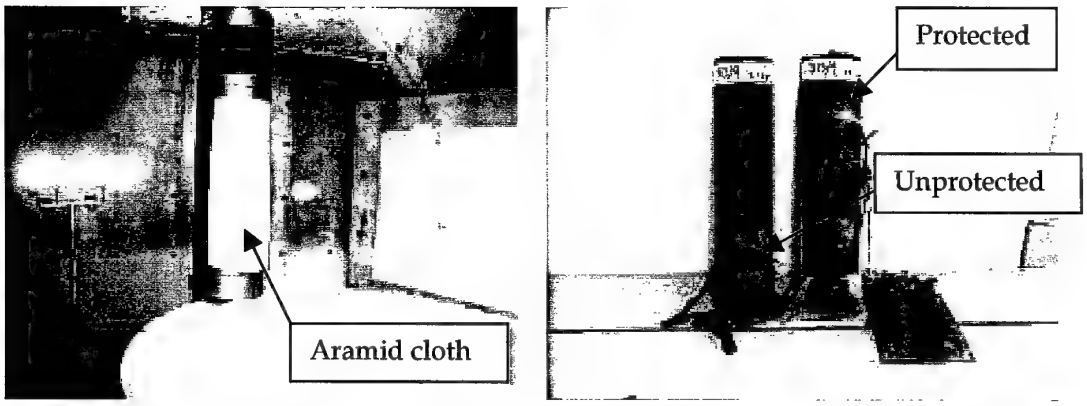

Figure 19. (Left) semi-cylinders of gelatine with skin were secured to the vertical members of the test rig; (Right) typical post-test result for semi-cylinders without and with protection.

4. Discussion and Conclusions

The injury potential of the PMN anti-personnel blast mine was assessed experimentally using a range of diagnostics including flash x-rays, break screens, fragmentation packs, and gelatine semi-cylinders. First, two mines were detonated in air to measure the maximum fragment velocity and maximum expansion rate of the detonation products that the mine could produce. Subsequent mine detonations where performed in soil, as the mine is designed to be used, in order to assess what effect this had on the mine blast and fragmentation output.

The detonation tests in air demonstrated that the PMN mine produces significant fragmentation due to the break up of the Bakelite case and the steel band that attaches the rubber cap and pressure plate to the main body of the mine. The steel band pieces that can have a mass up to 0.1 gram can reach a velocity of the order of 1100 m/s. They have a greater density and more aerodynamic shape, therefore producing a stronger penetration power than the Bakelite fragments, which have an average mass around 0.2 gram and can reach a velocity between 1400 and 1800 m/s. The Bakelite fragments appeared to be uniformly distributed across a ±20 degrees arc originating at the centre of the mine and about the horizontal plane parallel to the top and bottom of the mine. The steel band fragments were concentrated in the upper 5 degrees of this arc. Several fragments, originating from the pressure plate and the bottom of the mine are projected in the upward and downward vertical direction, respectively. The early expansion rate of the blast front is rapid with an initial velocity around 2000 m/s. This represents a significant blast overpressure for any object within 5 to 10 mine diameters from the mine.

Soil has a strong influence on the characteristics of the fragmentation and blast produced by the mine. The expansion rate of the detonation products was slowed down to around 900 m/s, which is specific to the depth of burial selected (20 mm overburden). Had the mine been buried deeper, the velocity of expansion would have been further reduced. In the immediate vicinity of the mine, the strong shock wave compressed the sand into a soft rock. It is unclear whether this is a characteristic of the particular sand used during these tests or a more general characteristic of soil. In any case, it appears that the soil directly above the mine formed a 'solid cap' that broke up soon after into smaller fragments. These fragments carried a lot of momentum and had a large damage potential. The damage to the aluminium bar located ~1.5 m above the soil surface could have been caused by these fragments or, as shown by the LS-Dyna computations, by the plastic plunger components. The impact craters were up to 15 mm in diameter and 5 to 6 mm deep. These impacts were registered within a cone that had an included angle of at least 30 degrees, which was defined from the length of the bar. The flash x-rays revealed that the initial velocity of the ejecta front was of the order of 800 to 900 m/s. The velocity of the front of soil particles was highest in the vertical direction and dropped rapidly with increasing angle about the vertical axis.

The results from in-soil detonations of PMN mines indicate that soil ejecta is a hazard for a contralateral leg that is placed 320 mm away from the mine. Examination of the gelatine semi-cylinders showed that the high-speed soil particles had an eroding effect on the leg surrogates, piercing the skin and eroding the underlying gelatine. For some tests, fragments from the mine case and from the steel band were embedded in the leg surrogates.

It was encouraging that simply adding a few layers of soft armour, such as Aramid cloth, could prevent soft tissue erosion. It is recommended that further work be done to design and build gaiter concepts that use soft armour materials. These gaiters should then be tested to assess their effectiveness for use in the field.

Acknowledgements

The authors would like to acknowledge their colleagues from the Terminal Effects group of DSTO Edinburgh for their support to set up and run the experiments discussed in this report. A special thank you is due to Dr J. Anderson, also from the Terminal Effects group, for contributing the LS-Dyna computations during the preparation of this report.

5. References

1. Jane's "Mines and Mine Clearance" Edited by Colin King 3rd Ed. 1998-99.
2. Bergeron, D.M., Walker, R.A. and Coffey, C.G., "Detonation of 100-Gram Anti-Personnel Mine Surrogate Charges in Sand", Report number SR 668, Defence Research Establishment Suffield, Canada, 1998.
3. Braid, M.P., *Experimental investigation and analysis of the effects of anti-personnel landmine blasts*, Thesis submitted to the Royal Military College of Canada, republished as DRDC Suffield SSP-2001-188, 2001.
4. Magnan, P. and Rondot, F., *Mapping of Air Overpressure around Surrogate AP Blast Mines*, Minutes of the AVT097/HFM102 RSM meeting, Koblenz, Germany, 2003.
5. Anatomical Surrogate Technologies, level 6, 19 North Terrace Hackney S.A. 5069 Australia, Director Wesley Fisk. 61 8132 1616.
6. RTO Technical Report TR-HFM-089, *Test Methodologies for Personal Protective Equipment Against Anti-Personnel Mine Blast*, NATO Research and Technology Organization, 2004.

Appendix A: Damage Report for Semi-Cylinders

The following excerpts are an integral reproduction from a letter report received from Anatomical Surrogate Technologies (AST). This company manufactured the gelatine semi-cylinders and inspected them after the tests.

A.1. Tests 313-5:

Unprotected target (Surrogate/TNT deflagration) in air initiation of PMN.

X-ray examination showed small particles embedded in the surrogate skin. Other fragments were found embedded in the anterior surface (below the surrogate skin) with associated skin roughening. Physical inspection showed tears in skin extending whole length of semi-cylinder. Major tear 15 cm from base with two larger tears centrally.

Possible repair (see note at end of Appendix)

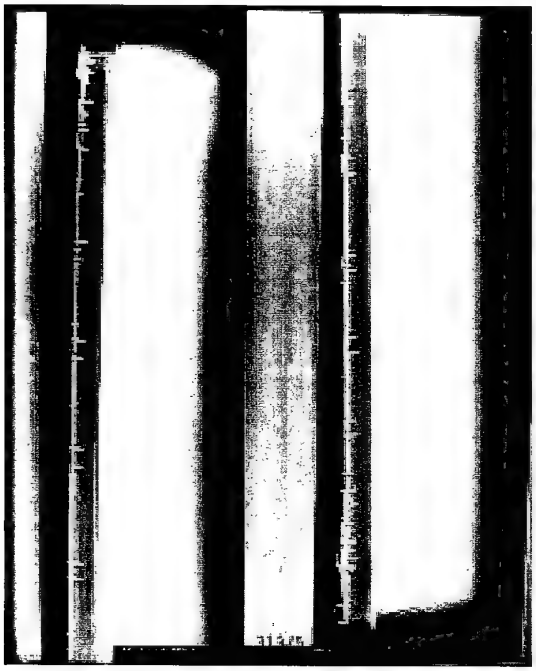

Overlapping side views of the unprotected semi-cylinder used in test 313-5 showing upper (left) and lower (right) extremities.

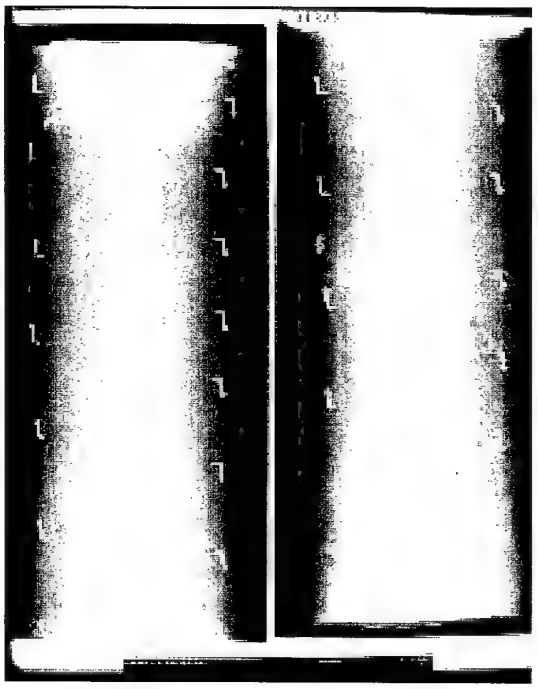

Overlapping front views of the unprotected semi-cylinder used in test 313-5 showing upper (left) and lower (right) extremities.

A.2. Tests 313-6:
Unprotected target (PMN/PE4 filled) in soil initiation of PMN

X-ray examination showed major damage to anterior surface. Surface roughening extending whole width of the cylinder. Radiolucent oval spots on entire surface. Physical examination showed tears in skin extending whole length of cylinder. Major tear 20 cm long near top of cylinder. Bottom tear may have underlying major soft tissue damage.

Possible repair (see note at end of Appendix)

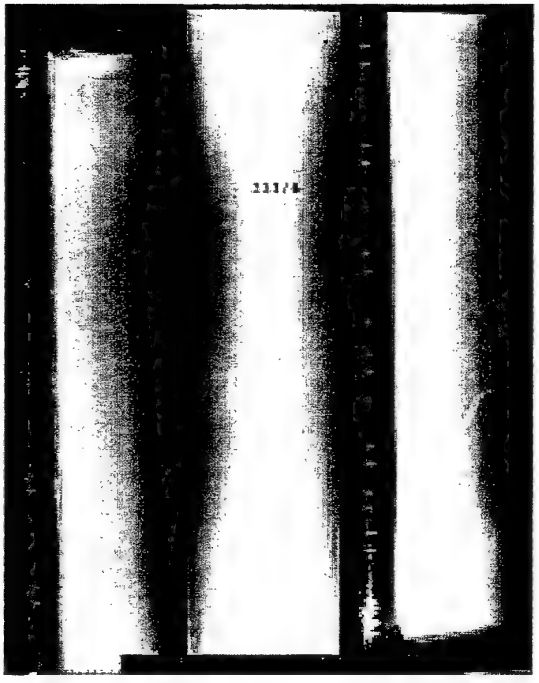

Overlapping side views of the unprotected semi-cylinder used in test 313-6 showing upper (left) and lower (right) extremities.

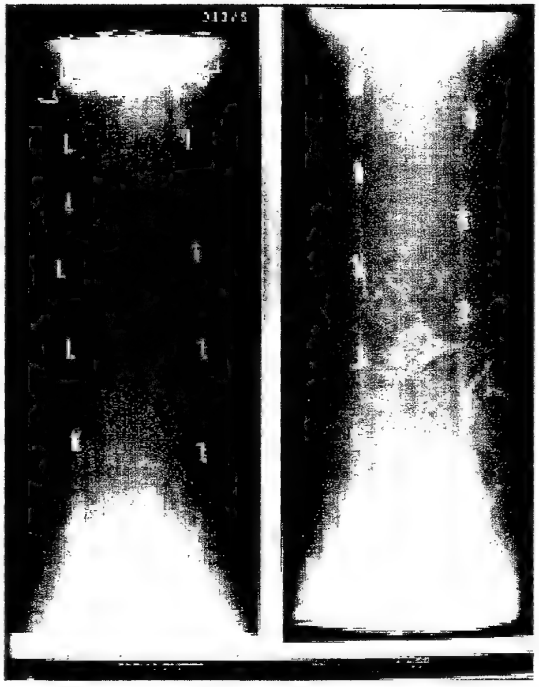

Overlapping front views of the unprotected semi-cylinder used in test 313-6 showing upper (left) and lower (right) extremities.

A.3. Tests 313-7:
Single unprotected target (PMN/PE4)

X-ray examination showed 6cm long area of damage near base extending the whole width of the cylinder. Query another area of damage 15cm above. Physical inspection showed major 15 cm tear in skin with underlying tissues affected. Smaller tears extending whole length of the cylinder. Deeper penetration into soft tissue at major tear.

Possible repair (see note at end of Appendix)

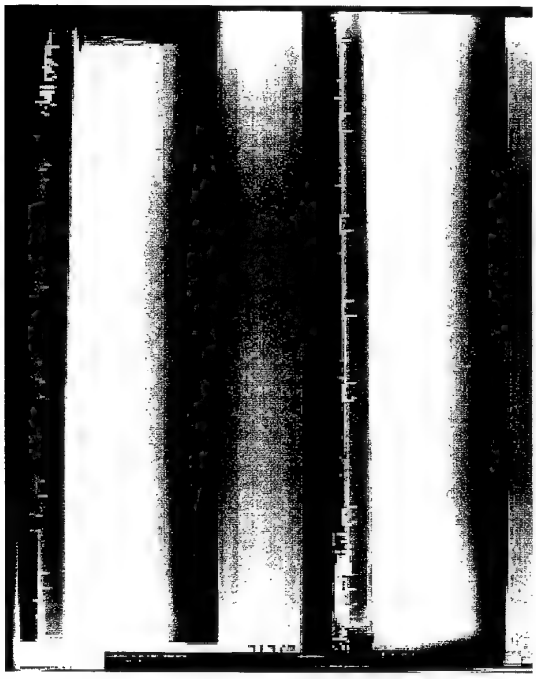

Overlapping side views of the unprotected semi-cylinder used in test 313-7 showing upper (left) and lower (right) extremities.

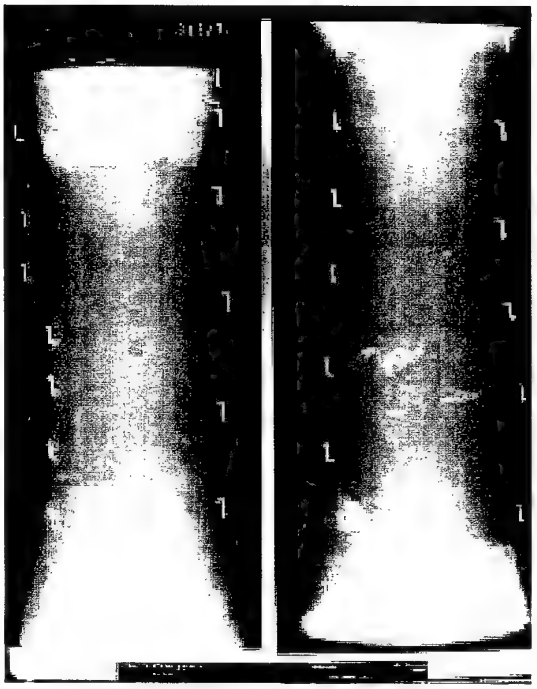

Overlapping front views of the unprotected semi-cylinder used in test 313-7 showing upper (left) and lower (right) extremities.

A.4. Tests 313-8:
Unprotected target (PMN/TNT)

X-ray examination showed small fragment embedded centrally on righ side with associated roughening of anterior surface. Anterior view shows small fragment. Physical inspection shows 5 cm wide tear and small tears 20 cm above base. Shrapnel embedded.

Possible repair (see note at end of Appendix)

Overlapping side views of the unprotected semi-cylinder used in test 313-8 showing upper (left) and lower (right) extremities.

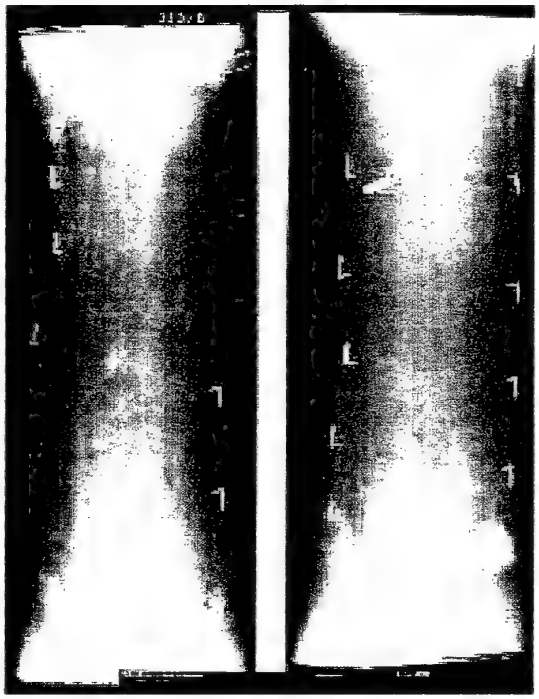

Overlapping front views of the unprotected semi-cylinder used in test 313-8 showing upper (left) and lower (right) extremities.

A.5. Tests 313-8:
Protected target (PMN/TNT)

X-ray examination showed no damage visible. Physical inspection showed no broken skin however the stocking had been damaged indicating possible blunt impact with associated friction.

Repairable

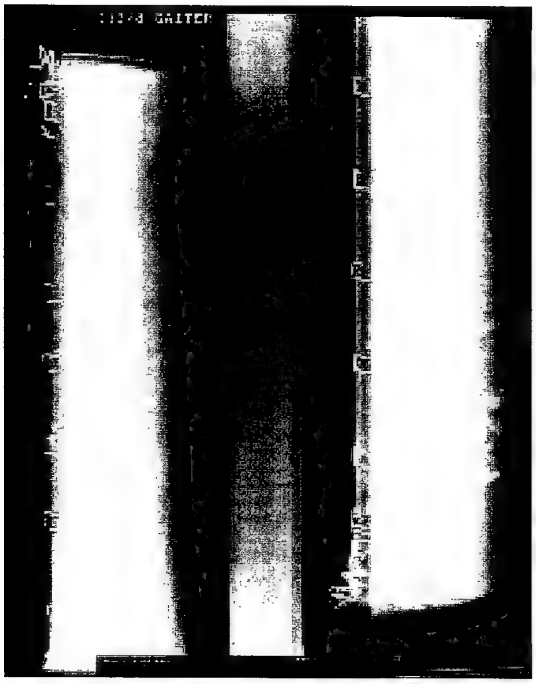

Overlapping side views of the protected semi-cylinder used in test 313-8 showing upper (left) and lower (right) extremities.

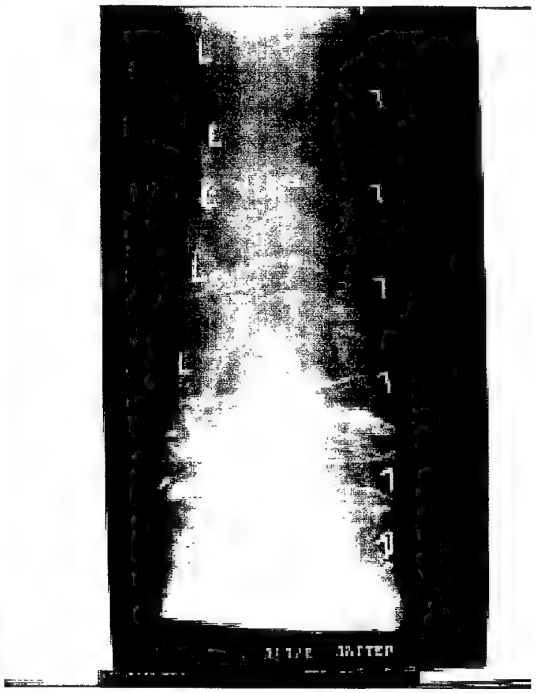

Overlapping front views of the protected semi-cylinder used in test 313-8 showing upper (left) and lower (right) extremities.

A.6. Tests 313-9:
Unprotected target (PMN/TNT)

X-ray examination showed extensive damage 10 cm above base across entire cylinder width. Physical inspection showed 5-7 cm long skin tear 10-15 cm from base across entire width. Small tears extend 20 cm above. Damage to underlying soft tissue central to major tear.

Possible repair (see note at end of Appendix)

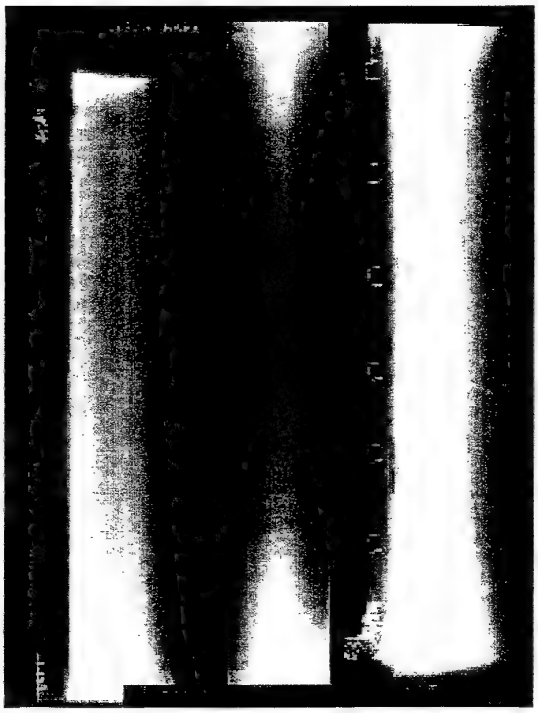

Overlapping side views of the unprotected semi-cylinder used in test 313-9 showing upper (left) and lower (right) extremities.

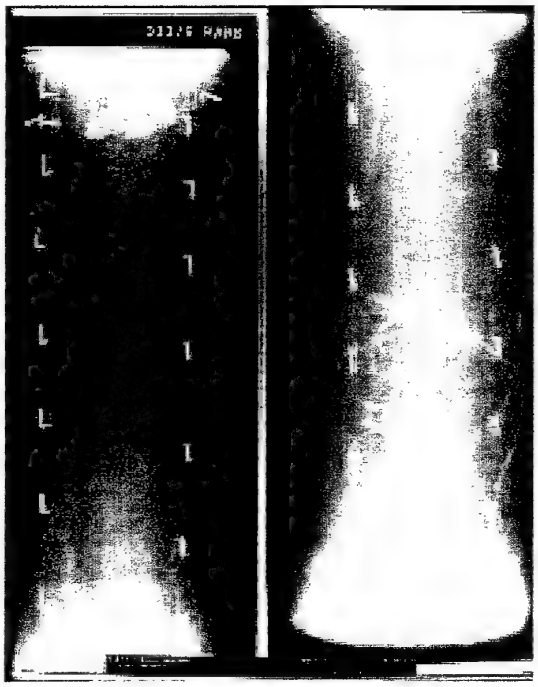

Overlapping front views of the unprotected semi-cylinder used in test 313-9 showing upper (left) and lower (right) extremities.

A.7. Tests 313-9:
Protected target (PMN/TNT)

X-ray examination showed no damage visible. Physical inspection showed small tear to skin above Kevlar line.

Repairable

Overlapping side views of the protected semi-cylinder used in test 313-9 showing upper (left) and lower (right) extremities.

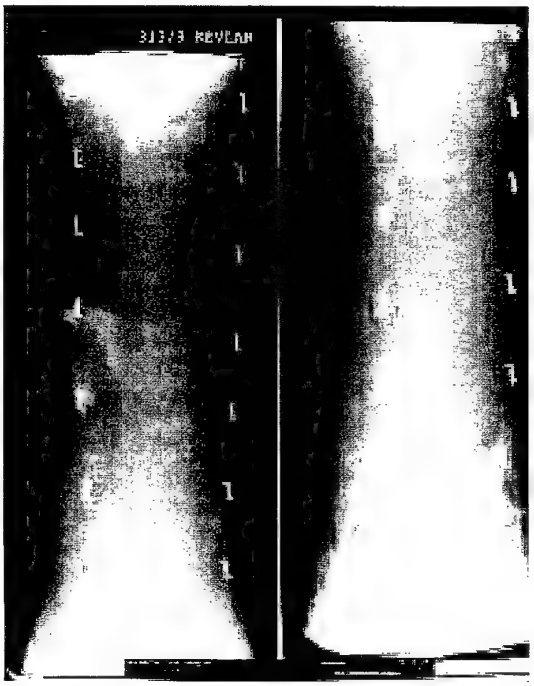

Overlapping front views of the protected semi-cylinder used in test 313-9 showing upper (left) and lower (right) extremities.

NOTE: Prof Henneberg would like to point out that due to the nature of the injuries shown on these gelatine cylinders (10-15 cm above base) and the corresponding close proximity of the tibia to the skin surface at this height, with full weight loading on the lower leg, there is a high probability that the tibia would have sustained some damage and possible fracture. AST would therefore caution the interpretation of these results as possible skeletal damage may have occurred even in those tests that did not show damage. He proposes that any future tests involve the use of FSLL's to better predict potential outcomes.

DISTRIBUTION LIST

Evaluation of a Silent Killer, the PMN Anti-Personnel Blast Mine

R.J. Swinton and D.M. Bergeron

AUSTRALIA

DEFENCE ORGANISATION

	No. of copies
Task Sponsor	
1 DGLD	2
S&T Program	
Chief Defence Scientist FAS Science Policy AS Science Corporate Management Director General Science Policy Development	shared copy
Counsellor Defence Science, London	Doc Data Sheet
Counsellor Defence Science, Washington	Doc Data Sheet
Scientific Adviser to MRDC, Thailand	Doc Data Sheet
Scientific Adviser Joint	1
Navy Scientific Adviser	1
Scientific Adviser - Army	1
Air Force Scientific Adviser	1
Scientific Adviser to the DMO M&A	1
Scientific Adviser to the DMO ELL	1
Systems Sciences Laboratory	
Chief of Weapon Systems Division	Doc Data Sht & Dist List
Research Leader Land Weapon Systems	Doc Data Sht & Dist List
Head CMT	1
Task Manager, Mr Roy Bird	1
Author(s):	
Mr R. Swinton	1
Dr D.M. Bergeron	1
Chief Combat, Protection and Nutrition Centre, Maribyrnong	1
Dr. Chris Anderson	1
DSTO Library and Archives	
Library Fishermans Bend	Doc Data Sheet
Library Maribyrnong	Doc Data Sheet
Library Edinburgh	1
Australian Archives	1
Capability Systems Division	
Director General Maritime Development	Doc Data Sheet
Director General Land Development	1
Director General Aerospace Development	Doc Data Sheet
Director General Information Capability Development	Doc Data Sheet

Office of the Chief Information Officer

Deputy CIO	Doc Data Sheet
Director General Information Policy and Plans	Doc Data Sheet
AS Information Strategies and Futures	Doc Data Sheet
AS Information Architecture and Management	Doc Data Sheet
Director General Australian Defence Simulation Office	Doc Data Sheet

Strategy Group

Director General Military Strategy	Doc Data Sheet
Director General Preparedness	Doc Data Sheet

HQAST

SO (Science) (ASJIC)	Doc Data Sheet

Navy

SO (SCIENCE), COMAUSNAVSURFGRP, NSW Doc Data Sht & Dist List
Director General Navy Capability, Performance and Plans, Navy Headquarters
Doc Data Sheet
Director General Navy Strategic Policy and Futures, Navy Headquarters
Doc Data Sheet

Army

Commander, Land Warfare Centre, Puckapunyal 1
SO (Science), Deployable Joint Force Headquarters (DJFHQ) (L), Enoggera QLD
Doc Data Sheet
SO (Science) - Land Headquarters (LHQ), Victoria Barracks NSW
Doc Data & Exec Summ

Intelligence Program

DGSTA Defence Intelligence Organisation 1
Manager, Information Centre, Defence Intelligence Organisation 1
Assistant Secretary Corporate, Defence Imagery and Geospatial Organisation
Doc Data Sheet

Defence Materiel Organisation

Head Airborne Surveillance and Control	Doc Data Sheet
Head Aerospace Systems Division	Doc Data Sheet
Head Electronic Systems Division	Doc Data Sheet
Head Maritime Systems Division	Doc Data Sheet
Head Land Systems Division	Doc Data Sheet
Head Industry Division	Doc Data Sheet
Chief Joint Logistics Command	Doc Data Sheet
Management Information Systems Division	Doc Data Sheet
Head Materiel Finance	Doc Data Sheet

Defence Libraries

Library Manager, DLS-Canberra	Doc Data Sheet
Library Manager, DLS - Sydney West	Doc Data Sheet

OTHER ORGANISATIONS

National Library of Australia	1
NASA (Canberra)	1

UNIVERSITIES AND COLLEGES

Australian Defence Force Academy	
Library	1
Head of Aerospace and Mechanical Engineering	1
Serials Section (M list), Deakin University Library, Geelong, VIC	1
Hargrave Library, Monash University	Doc Data Sheet
Librarian, Flinders University	1

OUTSIDE AUSTRALIA

INTERNATIONAL DEFENCE INFORMATION CENTRES

US Defense Technical Information Center	2
UK Defence Research Information Centre	2
Canada Defence Scientific Information Service	e-mail link to pdf
NZ Defence Information Centre	1

ABSTRACTING AND INFORMATION ORGANISATIONS

Library, Chemical Abstracts Reference Service	1
Engineering Societies Library, US	1
Materials Information, Cambridge Scientific Abstracts, US	1
Documents Librarian, The Center for Research Libraries, US	1

INFORMATION EXCHANGE AGREEMENT PARTNERS

Defence R&D Canada – Suffield, Major Braid, Canada	2

SPARES	5
Total number of copies:	**43**

DEFENCE SCIENCE AND TECHNOLOGY ORGANISATION
DOCUMENT CONTROL DATA

1. PRIVACY MARKING/CAVEAT (OF DOCUMENT)

2. TITLE

Evaluation of a Silent Killer, the PMN Anti-Personnel Blast Mine

3. SECURITY CLASSIFICATION (FOR UNCLASSIFIED REPORTS THAT ARE LIMITED RELEASE USE (L) NEXT TO DOCUMENT CLASSIFICATION)

Document	(U)
Title	(U)
Abstract	(U)

4. AUTHOR(S)

R.J. Swinton and D.M. Bergeron

5. CORPORATE AUTHOR

Systems Sciences Laboratory
PO Box 1500
Edinburgh South Australia 5111 Australia

6a. DSTO NUMBER	6b. AR NUMBER	6c. TYPE OF REPORT	7. DOCUMENT DATE
DSTO-TR-1582	AR-013-112	Technical Report	May 2004

8. FILE NUMBER	9. TASK NUMBER	10. TASK SPONSOR	11. NO. OF PAGES	12. NO. OF REFERENCES
E9505-28-28	ARM 01/044	DGLD	32	6

13. URL on the World Wide Web

http://www.dsto.defence.gov.au/corporate/reports/DSTO-TR-1582.pdf

14. RELEASE AUTHORITY

Chief, Weapons Systems Division

15. SECONDARY RELEASE STATEMENT OF THIS DOCUMENT

Approved for public release

OVERSEAS ENQUIRIES OUTSIDE STATED LIMITATIONS SHOULD BE REFERRED THROUGH DOCUMENT EXCHANGE, PO BOX 1500, EDINBURGH, SA 5111

16. DELIBERATE ANNOUNCEMENT

No Limitations

17. CITATION IN OTHER DOCUMENTS Yes

18. DEFTEST DESCRIPTORS

landmines, PMN, blast, fragmentation, survivability, measurements

19. ABSTRACT

The destructive output of the PMN mine was assessed experimentally by detonating actual mines in air and then in soil. The fragmentation pattern was recorded using a combination of flash X-rays, fragmentation packs, and gelatine cylinders. This made it possible to measure the velocity as well as the mass of the fragments, so that their injury potential could be estimated. This report describes the test set-ups and methodology used for the tests, and presents the results that were obtained.